

Investigation of biosorption behavior of red-254, a textile waste paint on activated sugar beet pulp

Demir F., Lacin O.*, and Sincar H.

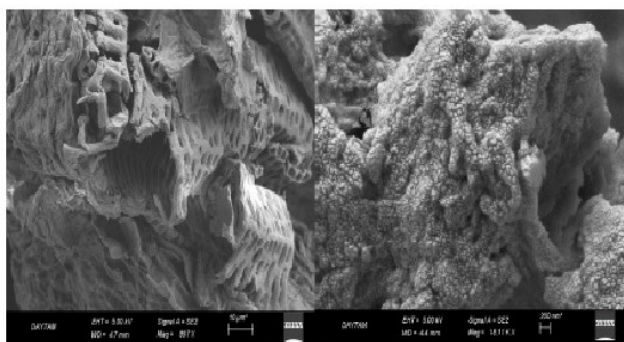
Ataturk University, Department of Chemical Engineering, Erzurum, Turkey

Received: 08/07/2021, Accepted: 24/11/2022, Available online: 14/12/2022

*to whom all correspondence should be addressed: e-mail: pchantzi@geo.auth.gr

<https://doi.org/10.30955/gnj.003872>

Graphical abstract



Abstract

In this study, activated sugar beet pulp as a biosorbent was used to remove Red-254 dye from aqueous solutions. The contact time, pH, biosorbent dosage and temperature were chosen as the parameters affecting the biosorption process. In the experiments, the batch adsorption technique was used. The isotherm, kinetic and thermodynamic parameters were calculated by using the data obtained from the experiments. The pseudo-second-order kinetic model and Langmuir isotherm model with $R^2 > 0.998$ in all cases were individually fitted to experimental data. The maximum monolayer biosorption capacity was found to be 84.75 mg.g^{-1} . Additionally, from the positive values of ΔH° and the negative values of ΔG° , it can be expressed that biosorption processes were carried out with endothermic, physical adsorption, spontaneous and thermodynamically favorable. As a result, the sugar beet pulp, which can be found as waste from the sugar factories, can be used as biosorbent for the removal of Red 254 dye from aqueous solutions.

Keywords: Biosorption, red-254, sugar beet pulp, isotherm models, kinetic models, thermodynamic parameters.

1. Introduction

In industrial plants such as tanning, dyeing, textile, cosmetics, plastic, food etc., it is assumed that more than a thousand organic dyes are commercially available. Among them, azo-based paints constitute approximately 70% of the total paints. There are also unwanted heavy metal ions in their content. Industrial discharge of these types of dyes into the ecosystem causes serious risks living to things (Yusuf *et al.*, 2021; Wanyonyi *et al.*, 2014; Kalkan *et al.*, 2012; Pitsari *et al.*, 2013; Altundogan *et al.*, 2007; Akar *et al.*, 2010). Therefore, the concentration of dyes must be reduced to the desired value before discharge to the receiver medium of dyestuffs in wastewater (Rathi *et al.*, 2021; Khattri and Singh, 2009).

Many chemical and physical dye-removal methods, including such as photocatalytic degradation (Joseph *et al.*, 2009), membrane filtration (Zhu *et al.*, 2017), precipitation (Gunduz and Bayrak, 2017), ion exchange (Reynier *et al.*, 2015) and adsorption techniques (Ngah *et al.*, 2011) have been used. It is stated that the adsorption technique is superior to the other removal techniques since it is economically low-cost and simple. In the adsorption process, many adsorbents have been used to remove dyes (Yagub *et al.*, 2014; Rafatullah *et al.*, 2010).

Activated carbon is one of the most commonly used adsorbents in wastewater treatment in the world. Because, it has superior properties such as porous structure, high adsorption capacity and large surface area (Imamoglu and Tekir, 2008; Lafta *et al.*, 2014). However, in recent years, new adsorbent materials have been employed in adsorption processes instead of activated carbon. These adsorbents attract the attention of researchers because of their low cost, abundance, and eco-friendly features in wastewater treatment (Yao *et al.*, 2011; Lacin *et al.*, 2019; Foroughi-Dahr *et al.*, 2015; Altundogan, 2005; Salazar-Rabago *et al.*, 2017; Akar *et al.*, 2016; Wang *et al.*, 2008; Kavci, 2020; Amri *et al.*, 2019; Tay *et al.*, 2020; Tran *et al.*, 2017). Biosorption commonly used to remove dyes from wastewater is one of the simple, low-cost, effective and ecological techniques. Various biomaterials such as natural residues, agricultural

wastes, bacteria, fungi, microalgae etc. are used as biosorbent in the removal of dyes (Danouche *et al.*, 2021). Therefore, in this study, it has been investigated whether activated sugar beet pulp (ASBP), which is found as waste in sugar production from sugar beet, can be used as a biosorbent. For this purpose, ASBP is used to investigate the biosorption behavior of R-254 dyestuff from aqueous solutions. The effect of the contact time, the initial concentration, the temperature, the pH and the biosorbent mass on biosorption process are investigated. The biosorption kinetics, thermodynamics and equilibrium studies are conducted by batch adsorption technique.

2. Materials and methods

2.1. Materials

In this study, the solutions of pigment R-254 supplied from Ozcanlar Textil Ltd. Şti. in Istanbul/Turkey were used as dyestuff and it was prepared by distilled water. R-254 is

Table 1. Some properties of R-254

CAS no	84632-65-5
IUPAC name	1,4-bis(4-chlorophenyl)-2,5-dihydropyrrolo[3,4-c]pyrrole-3,6-dione
Molecular Weight (g.mol ⁻¹)	357.19
Molecular Formula	C ₁₈ H ₁₀ Cl ₂ N ₂ O ₂
Ph Value	7
Density (g/ml)	1.5
Water Solubility (mg/L)	4.10 ⁴ (25 °C)
Oil Absorption(ml/100g)%	40
Light Fastness	8
Heat Resistance	250 (°C)
Water Resistance	5
Oil Resistance	5
Acid Resistance	5
Alkali Resistance	5
λ _{max} (nm)	543

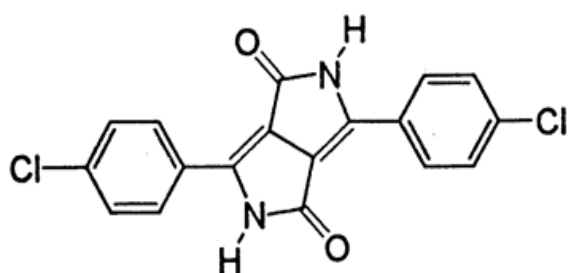


Figure 1. Chemical structure of R-254

2.2. Biosorption studies

The R-254 biosorption onto ASBP was performed using a batch adsorption technique. In these studies, the initial concentration, the contact time, the temperature, the solution pH and the biosorbent dosage were selected as dependent parameters and parameter values were given in Table 3.

an anionic, bright red, heterocyclic organic pigment with excellent heat resistance. Some thermo-physical properties of R-254 are presented in Table 1. The chemical structure of R-254 is given in Figure 1.

The sugar beet pulp (SBP) provided as waste product by Erzurum Sugar Factory was used as biosorbent. It was sieved through 0.517-0.27 μm sieved, washed with distilled water and then dried overnight at 85 °C. Some properties of wet and dry sugar beet pulp are given in Table 2. At 85 °C, it was activated for 6 hours with the solid/liquid ratio of 1 g dry SBP/125 ml of 0.7 M HNO₃ acid solution. Then, the solution was centrifuged to separate the ASBP. It was washed several times with distilled water until the pH was neutral. Then, it was placed in an oven at 85 °C and dried until it reached a constant weight. All other chemicals used were of analytical purity.

The pH values were adjusted with a digital pH meter (model Thermo Orion 3 Star pH meter) using 0.1 M NaOH and 0.1 M HCl solutions. Biosorption experiments were carried out in a temperature-controlled shaker (Edmund Bühler GmbH KS-15) at a constant mixing speed of 225 rpm according to the given values in Table 3. At the end of each experimental work, some samples were taken from the final solution and centrifuged immediately at 5000 rpm for 10 minutes (model Nuve NF 1215) and then the solution was separated from the solid. R-254 concentration was found by a Thermo Evolution 500 UV spectrophotometer by using a calibration curve at the maximum wavelength corresponding to R-254 (543 nm).

The removal percentage of R-254 was calculated using Equation 1.

$$\text{R-254 Removal \%} = \frac{(C_0 - C_t)}{C_0} \times 100 \quad (1)$$

where C₀ (mg.L⁻¹) and C_t (mg.L⁻¹) are the R-254 concentrations at the initial and time t, respectively.

Table 2. Properties of wet and dry sugar beet pulp

Ingredients	wet %	dry %
Water	75.84	-
Sucrose	17.1	70.7
Pectin	2.2	9.4
Raw oil	0.1	0.4
Raw cellulose	2.1	8.9
Nitrogenous substances	1.1	4.6
Ash	1.06	4.5
Other	0.3	1.5

Table 3. Selected biosorption parameters and values

Parameters	Values
Initial Concentration (mg.L ⁻¹)	25 - 50* - 75 - 100
Contact Time (min.)	1 - 5 - 10 - 30 - 60 - 120* - 180
Temperature (°C)	25* - 30 - 35 - 40 - 45 - 50
pH	2 - 4 - 5.69* - 6 - 8 - 10
Biosorbent Dosage (g.L ⁻¹)	0.25 - 0.5* - 1.0 - 1.5 - 2

Biosorption capacity at equilibrium, q_e (mg.g⁻¹) evaluated from the initial (C_0) and equilibrium (C_e) R-254 concentrations (mg.L⁻¹) in the solution is computed by Equation 2:

$$q_e = (C_0 - C_e) \frac{V}{m} \tag{2}$$

where V (L) is the solution volume and m (g) is the ASBP dosage.

2.3. Characterizations

The ASBP was analyzed by X-ray diffraction using Rigaku 2200D/Max, X-ray diffractometer, Cu K α ($\lambda = 1.5405 \text{ \AA}$) radiation in the 2 θ range 0-50° was used.

The surface morphology was analyzed by A ZEISS SIGMA 300 Scanning Electron Microscopy (SEM). The contact angle was measured by Attension Theta Flex. Particle size and zeta potential analysis was performed by Malvern Zetasizer Nano ZSP.

With Micrometrics 3Flex device, surface area analysis with Brunauer-Emmett-Teller (BET) and pore size-volume analysis with Barrett-Joyner-Halenda (BJH) were carried out.

2.4. Adsorption isotherm, kinetics and thermodynamic equations

Adsorption isotherms play an important role in the design of an adsorption stem to remove the substance to be adsorbed from solutions. There is a dynamic equilibrium in the interaction between the adsorbate and the adsorbent in the adsorption process. The equilibrium data must be analyzed for the development of mathematical models. These equilibrium models present important information about adsorption mechanisms, affinities of the adsorbent and surface properties. Different isotherm models are available to analyze the experimental data. However, the most popular isotherm models used in adsorption processes in aqueous solutions are Freundlich, Langmuir, Temkin and Dubinin-Radushkevich (D-R) models

(McKay *et al.*, 1999; Reddad *et al.*, 2002; Fathi *et al.*, 2015; Castro *et al.*, 2017; Pehlivan *et al.*, 2008).

The Langmuir isotherm describes that a monolayer of adsorbent occurs over homogenous sites on the adsorbent. The dimensionless equilibrium parameter values (R_L) indicate the type of the isotherm (unfavorable ($R_L > 1$) linear ($R_L = 1$), favorable ($0 < R_L < 1$) or irreversible ($R_L = 0$)).

Freundlich isotherm is an empirical equation, which indicates that the adsorption process takes place on a heterogeneous surface. Adsorption capacity is related to the concentration of dye at equilibrium. If n value in the formula is between 1 and 10, the adsorbent is suitable for adsorption.

The Temkin isotherm is an empirical equation and it explains interactions between the adsorbate and the adsorbent in the adsorption process. It is characterized by a homogenous distribution of binding energies.

The Dubinin Radushkevich isotherm is generally applied to describe the adsorption mechanism and nature with a Gaussian energy distribution onto a heterogeneous surface.

It is very important to examine the kinetics to determine which of the adsorption mechanism of the system is controlled. In this study, Elovich, Pseudo-First-Order, Pseudo-Second-Order and intra-particle diffusion models were applied (Bulut and Aydin, 2006; Li *et al.*, 2016; Nuhanović *et al.*, 2019). Experimental adsorption isotherm and kinetic models were compared with the models given in Tables 4 and 5, respectively.

The thermodynamic parameters such as the Gibbs free energy change (ΔG° , kJ.mol⁻¹), the enthalpy change (ΔH° , kJ.mol⁻¹) and the entropy change (ΔS° , kJ.mol⁻¹) were calculated to confirm the nature of the biosorption process.

Table 4. The isotherm models commonly used in aqueous solutions

Isotherms	Mathematical Equations	Equations
Langmuir	$\frac{C_e}{q_e} = \frac{C_e}{q_m} + \frac{1}{K_L \times q_m} R_L = \frac{1}{1 + K_L C_0}$	Eq. 3
Freundlich	$\ln(q_e) = \ln(K_f) + \frac{1}{n} \times \ln(C_e)$	Eq. 4
Temkin	$q_e = R_g T / b_T \times \ln(K_T C_e)$	Eq. 5
D-R	$\ln(q_e) = \ln(q_m) + \beta \times \varepsilon^2 \quad \varepsilon = R_g T \ln\left(1 + \frac{1}{C_e}\right)$	Eq. 6

Table 5. The kinetic models tested experiments

Isotherms	Mathematical Equations	Equations
Pseudo First Order	$\log(q_e - q_t) = \log(q_e) - k_1 \times t$	Eq. 7
Pseudo Second Order	$\frac{t}{q_t} = \frac{1}{k_2 \times q_e^2} + \frac{t}{q_e}$	Eq. 8
Elovich	$q_t = \frac{\ln(\alpha\beta)}{\beta} + \frac{\ln t}{\beta}$	Eq. 9
Intraparticle diffusion	$q_t = k_{dif} \times t^{\frac{1}{2}} + C$	Eq. 10

ΔG° can be found with Van't Hoff Equation 11. If ΔG° value is a negative quantity, the reaction occurs spontaneously. In physical adsorption, ΔG° varies between -20 and 0 kJ.mol⁻¹. In chemical adsorption, it is between -80 and -400 kJ.mol⁻¹ (Agarry and Ogunleye, 2014).

$$\Delta G^\circ = -R_g T \times \ln(K_0) = \Delta H^\circ - T\Delta S^\circ \quad (11)$$

With the modification of Equation 11 is obtained Equation 12 as follows:

$$\ln(K_0) = (\Delta S^\circ / R_g) - (\Delta H^\circ / R_g T) \quad (12)$$

K_0 is the equilibrium constant; R_g is the universal gas constant (8.314 J.(mol.K)⁻¹); and T is the absolute temperature (K). Also, K_0 is calculated from Equation 13 as follows (Zhou *et al.*, 2022):

$$K_0 = 10^6 \times K_L \quad (13)$$

ΔH° and ΔS° parameters are calculated from Equation 12. The value of ΔH° also determines whether the adsorption process is physical (80<kJ.mol⁻¹) or chemical (80-200 kJ.mol⁻¹) (Agarry and Ogunleye, 2014).

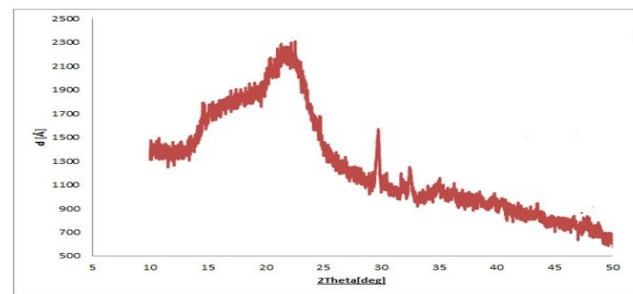
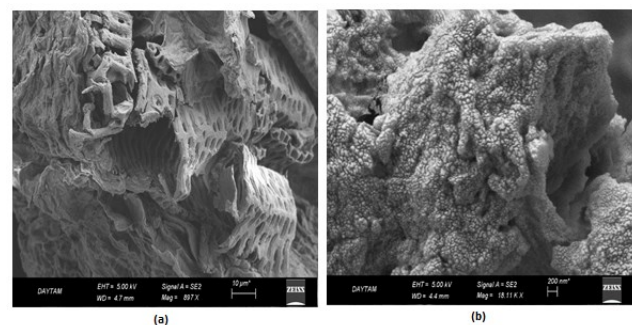
3. Results and discussion

3.1. ASBP characterization

X-ray diffraction (XRD) patterns of ASBP are shown in Figure 2. The major diffraction intensities at 15°, 23° and 30° 2θ indicate that ASBP sample is of the typical cellulose I structure.

Scanning Electron Microscopy (SEM) images before and after biosorption of ASBP are shown in Figure 3. It can be seen from Figure 3a that the biosorbent has a rough and heterogeneous porous structure. It can also be seen from

Figure 3b that the dye molecules are to be adsorbed onto the surface of the biosorbent.

**Figure 2.** Typical XRD pterns of ASBP**Figure 3.** a and b SEM micrograph of ASBP before and after biosorption, respectively

Particle size analysis of ASBP dried, milled and sieved is given in Figure 4. It is obvious from Figure 4, it gives 531 nm in the first peak, 459 nm in the second peak and 615 nm in the third peak. The average particle size is calculated as 535 nm.

The R-254 surface analysis results are given in Figure 5 and Table 6.

Table 6. The ASBP surface analysis results

Surface Area (S, m ² .g ⁻¹)	Pore Volume(Vp, cm ³ .g ⁻¹)	Average Pore Size(dp nm)
29.41	0.03509	4.7736

The equilibrium contact angle shows the hydrophilicity of a solid surface by a liquid via the Young equation. Additionally, it reflects the relative strength of the liquid, solid, and vapour molecular interaction. The smaller the equilibrium contact angle from 90°, the higher the hydrophilicity property. As a result, the biosorption capacity of the biosorbent will increase. The equilibrium contact angle is shown in Figure 6. It is clear from Figure 6 that the biosorption capacity of the biosorbent is high since the equilibrium contact angle is about 67°.

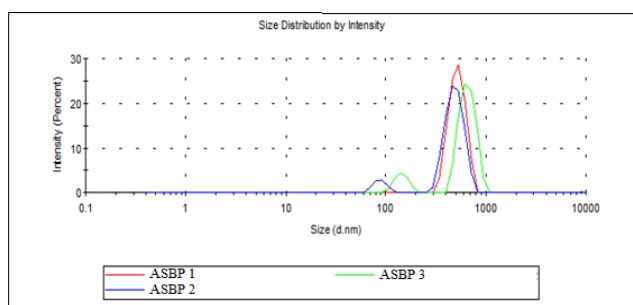


Figure 4. Particle size analysis of ASBP

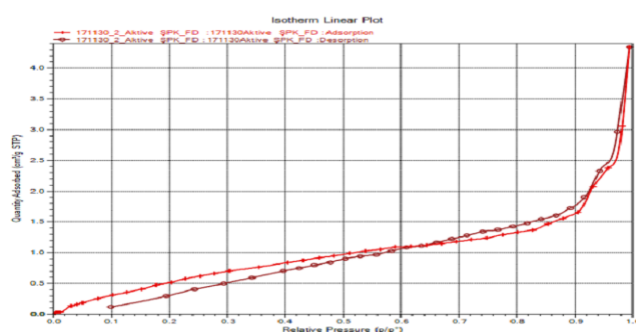


Figure 5. Biosorption isotherm of nitrogen at 77 K for ASBP

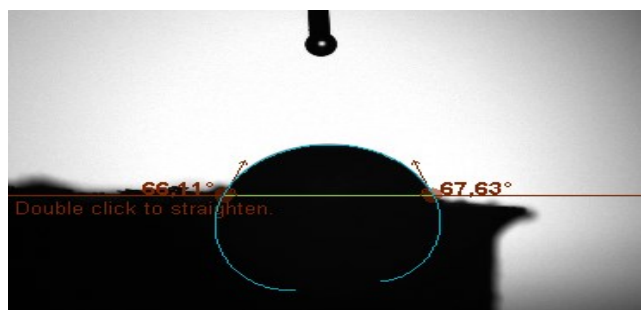


Figure 6. The equilibrium contact angle of ASBP

3.2. Effect of initial concentration and contact time on the biosorption capacity

To determine the biosorption equilibrium time, the batch adsorption process was carried out at the contact times and the different initial concentrations. Figure 7 was

drawn using the data obtained at the end of the experiment. As can be seen from Figure 7, the biosorption rate is high at the beginning of the process and then it starts to decrease gradually. Eventually, the biosorption rate reaches the equilibrium condition. The equilibrium time for this biosorption process is determined as approximately 120 minutes. In all other experiments, the contact time is taken as 120 minutes.

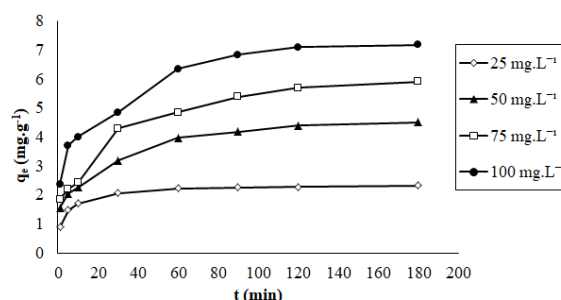


Figure 7. Determination of equilibrium time (the initial solution pH 5.69, biosorbent dosage 0.5 g, temperature 25 °C, stirring speed 225 rpm, R-254 concentrations 25-100 mg.L⁻¹)

3.3. pH effect on the biosorption capacity

The solution pH is the most important parameter governing the dye biosorption process since it affects the biosorption capacity. The zero charge point (pH_{zpc}) corresponds to the pH value at which the biosorbent surface is considered to be neutral. It plays an important role in explaining the adsorption of ionic species on biosorbent surfaces in aqueous systems. The determination of pH_{zpc} of ASBP was performed (Zou and Zhao, 2012). The value of pH_{zpc} can be determined from the curve that cuts the pH_i line of the plot ΔpH versus pH_i (Figure 8). The pH_{zpc} point of ASBP was determined as 6.62 and the pK_a value of R-254 was found to be 8.46 from the literature (Chemical book 2016). When the pH value of the dye solution is lower than 6.62, ASBP behaves positively charged and when the pH value is higher than 6.62, ASBP behaves negatively charged. On the other hand, when the pH value of the dye solution is less than 8.46, the R-254 adsorbate behaves negatively charged and when the pH value is greater than 8.46, it behaves positively charged.

The biosorption of R-254 dyes onto ASBP was determined by changing the pH in the range of 2.0–10.0 and given in Figure 9. As can be seen from Figure 9, while the biosorption capacity increases at pH 2-6, it decreases at pH 6-10.

It can be said that the increase in biosorption capacity at low pH values is due to the electrostatic attraction forces between the positively charged ASBP biosorbent and the

negatively charged R-254, while the decrease at high pH values is due to the repulsive forces between the biosorbent surface functional groups and the dye molecules interacting. So, in the experimental studies, the initial solution pH value of 5.69 was chosen as the constant parameter.

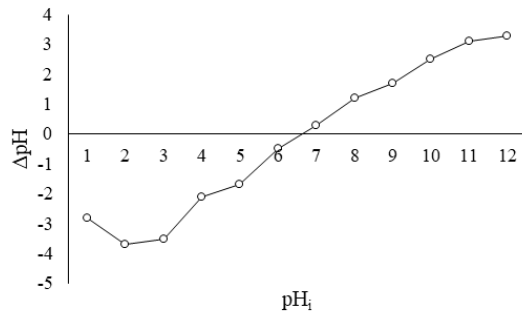


Figure 8. pHzpc of ASBP.

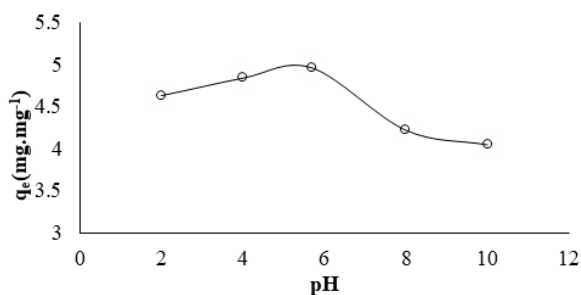


Figure 9. Determination of suitable pH (contact time 120 min, biosorbent dosage 0.5 g.L⁻¹, temperature 25 °C, stirring speed 225 rpm, R-254 concentrations 50 mg.L⁻¹)

3.4. ASBP dosage effect

The biosorbent dosage on the removal of R-254 provides a high contribution due to the number of available active sites on the surface of biosorbent. Therefore, the effect of biosorbent dosage was examined by varying it in the range 0.25 to 2.0 g.L⁻¹ and the results are given in Figure 10. It can be clearly seen from Figure 10 that the biosorption capacity (q_e) decreases and biosorption percent increases with the increasing value of the ASBP dosage from 0.25 to 2.0 g.L⁻¹. An increase in the biosorption percent is due to the increase in the biosorbent surface and hence, more active functional groups result in the availability of more biosorption sites. Additionally, the biosorption capacity decreases by increasing the biosorbent dosage due to the unsaturated biosorption site numbers during the biosorption process (Malekbala *et al.*, 2012). The biosorbent dosage of 0.5 g.L⁻¹ was selected next experiments.

3.5. Analysis of the biosorption isotherms

Four isotherm models presented in Table 4 were investigated the biosorption process mechanism in the removal of R-254 from aqueous solution by using ASBP as biosorbent. From Equation 3, when the C_e versus C_e/q_e is plotted, Langmuir constants (q_m and K_L) are found from the intercept and slope of a linear relation. The other isotherm constants in Equations 4-6 are calculated in the same way. Isotherm parameters and R^2 values obtained by applying experimental data to equilibrium isotherm models are given in Table 7 and Figure 11.

Table 7. Isotherm parameters and R^2 values of equilibrium isotherm models for the R-254 biosorption onto ASBP at 25 °C

Isotherm parameters	R-254 Dye
Langmuir	
q_m (mg.g ⁻¹)	84.75
$K_{L,25^\circ C}$ (L.mg ⁻¹)	0.16
$K_{L,30^\circ C}$ (L.mg ⁻¹)	0.13*
$K_{L,35^\circ C}$ (L.mg ⁻¹)	0.12*
$K_{L,40^\circ C}$ (L.mg ⁻¹)	0.09*
$K_{L,45^\circ C}$ (L.mg ⁻¹)	0.08*
$K_{L,50^\circ C}$ (L.mg ⁻¹)	0.07*
R_L	0.93
R^2	0.99
Freundlich	
$K_f [(\text{mg.g}^{-1}) (\text{L.mg}^{-1})^{-1/n}]$	2.70
n	0.43
R^2	0.96
Temkin	
K_T (L.mg ⁻¹)	9.34
B_T	18.19
R^2	0.98
Dubinin-Radushkevich	
$\beta_{DR} (\times 10^{-6} \text{mol}^2 \cdot \text{kJ}^{-2})$	1
q_m (mg.g ⁻¹)	4.13
R^2	0.93

* K_L values at other temperatures are added to the table to calculate K_0 .

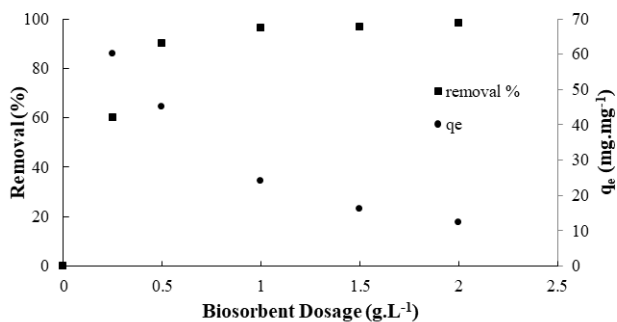


Figure 10. Effect of biosorbent dosage (contact time 120 min, the initial solution pH 5.69, temperature 25 °C, stirring speed 225 rpm, R-254 concentrations 50 mg.L⁻¹)

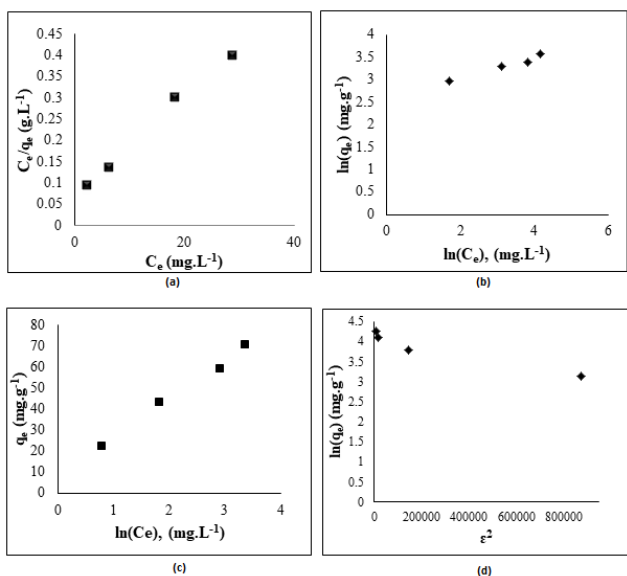


Figure 11. Isotherm curves for different isotherms models (a-Langmuir, b-Freundlich, c-Temkin, d-D-R) (contact time 120 min, the initial solution pH 5.69, temperature 25 °C, stirring speed 225 rpm)

Biosorption process of R-254 onto the ASBP is favorable because the R-value is in the range of 0-1. At the same time, if the n value is greater than 1, it can be stated that ASBP is a suitable biosorbent for R-254 biosorption. From Table 7 and Figure 11, at 25 °C, the isotherm model best suited to the biosorption of R-254 on ASBP is found to be Langmuir with R² value of 0.99. Similar results are reported in the literature (Vučurović *et al.*, 2012; Pehlivan *et al.*, 2006).

3.6. Analysis of the biosorption kinetics

The applicability of four well-known kinetic models presented in Table 5 was estimated through the kinetic parameters, equilibrium biosorption capacity and correlation coefficients shown in Table 8. From Equation 7, when log(q_e-q_t) versus t is plotted (Figure 12), pseudo-first-order constants (k₁ and q_e) are found from the intercept and slope of a linear relation. The kinetic constants in Equations 8-10 are calculated in the same way. The R² and kinetic constants were obtained by

applying experimental data to kinetics models given in Table 8 and Figure 12.

When Table 8 and Figure 12 are examined, the kinetic model corresponding to the experimental data is a pseudo-second-order model. The correlation coefficient of the pseudo-second-order kinetic model is relatively high (0.996–0.999).

Similar kinetic results are reported in the removal of dyes from an aqueous solution by using SBP as biosorbent (Harifi-Mood and Hadavand-Mirzaie, 2015; Aksu and Isoglu, 2005).

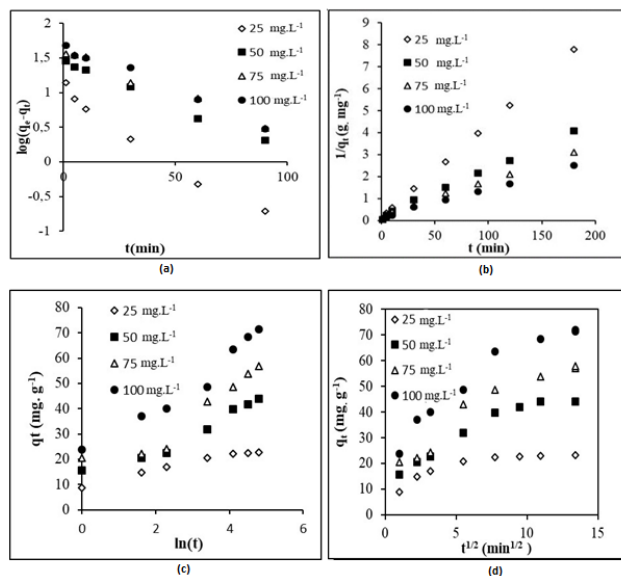


Figure 12. Kinetics curves for different kinetics models (a-Pseudo-first-order, b-Pseudo-second-order, c-Elovich, d-Intraparticle diffusion) (biosorbent dosage 0.5 g.L⁻¹, the initial solution pH 4.59, temperature 25 °C, stirring speed 225 rpm)

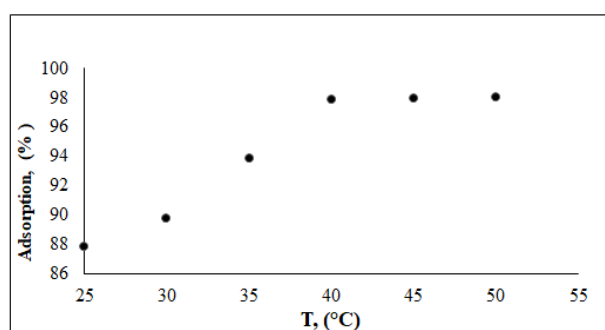


Figure 13. Effect of temperature on the biosorption of R-254 dye by ASBP (biosorbent dosage 0.5 g, the initial solution pH 4.59, temperature 25 °C, stirring speed 225 rpm)

3.7. Biosorption thermodynamics and temperature studies

The effect of temperature on the biosorption of R-254 onto ASBP from aqueous solution is estimated by variation of the temperature in the range from 298 to 323 K (Figure 13). It can be seen in Figure 13 that the removal

of R-254 onto ASBP was slightly increased with the increasing temperature from 298 to 323 K. This situation

may be due to interactions between biosorbent and adsorbate and the creation of new biosorption sites.

Table 8. Comparison of the kinetic models for R-254 dye concentrations of at 25 °C

a		Pseudo First Order				Pseudo Second Order			
Dye	$C_o(\text{mg.L}^{-1})$	$q_{e,\text{exp}}(\text{mg.g}^{-1})$	$k_1(\text{min}^{-1})$	$q_{e,\text{cal}}(\text{mg.g}^{-1})$	R^2	$k_2(\text{g.mg}^{-1}.\text{min}^{-1})$	$q_{e,\text{cal}}(\text{mg.g}^{-1})$	R^2	
R-254	25	22.82	0.05	10.43	0.978	0.01	23.34	0.998	
	50	43.92	0.03	28.52	0.989	0.01	35.09	0.999	
	75	56.89	0.03	38.93	0.970	0.02	59.84	0.999	
	100	71.36	0.03	45.76	0.986	0.02	74.08	0.996	

b		Elovich			Intraparticle Diffusion			
Dye	$C_o(\text{mg.L}^{-1})$	$q_{e,\text{exp}}(\text{mg.g}^{-1})$	$\alpha(\text{g.mg}^{-1})$	$\beta(\text{mg.g}^{-1}.\text{dk}^{-1})$	R^2	$k_{\text{dif}}(\text{mg.g}^{-1}.\text{min}^{-1/2})$	C	R^2
R-254	25	22.82	76.63	0.33	0.98	1.01	12.31	0.960
	50	43.92	41.95	0.16	0.95	1.02	15.79	0.930
	75	56.89	40.02	0.12	0.89	1.03	18.51	0.930
	100	71.36	77.73	0.10	0.86	1.04	27.66	0.930

From E, when the plot $1/T$ versus $\ln K_c$ is plotted (Figure 14), the values of ΔH° and ΔS° are found from the intercept and slope of linear relation and then used to calculate ΔG° according to Equation 11. The thermodynamic parameters for biosorption of R-254 onto ASBP are presented in Table 9.

The positive value of ΔH° ($72.65 \text{ kJ.mol}^{-1}$) shows that the biosorption process of R-254 onto ASBP is endothermic, which means the hydration energy is partly compensated in the release of biosorption energy. Additionally, the ΔH° magnitude shows the physical of the biosorption process.

The positive value of ΔS° (260 J.mol^{-1}) for the ASBP indicates an increase in irregularity among the R-254 biosorption molecules for the active sites of the ASBP surface at the solid-liquid interface.

The negative ΔG° values ($4.76\text{-}11.25 \text{ kJ.mol}^{-1}$) indicate a favorable and spontaneous removal process of R-254 onto ASBP at all the experimental temperatures. In addition, the biosorption process is found to be carried out by

Table 9. Thermodynamic parameters for the biosorption of R-254 on ASBP

$\Delta H(\text{kJ.mol}^{-1})$	$\Delta S(\text{J.mol}^{-1})$	$\Delta G(\text{kJ.mol}^{-1})$			
T (K) 298	89.8	298	303	308	313
		318			
		323			
2.7	89.8	-2.67	-2.72	-2.76	-2.81
		-2.85			
		-2.90			

4. Conclusions

The activated form of sugar plant waste, sugar beet pulp, was used as biosorbent to remove R-254 from its aqueous solutions. In the characterization studies of the ASBP, it is observed that there has a rough and heterogeneous porous structure. The average particle size is calculated as 535 nm. It was determined that the ASBP is to be used as biosorbent since the equilibrium contact angle is about 67 °. It is observed that R-254 biosorption increased with

physical adsorption, since the values of ΔG° are in the range of physical adsorption in this study.

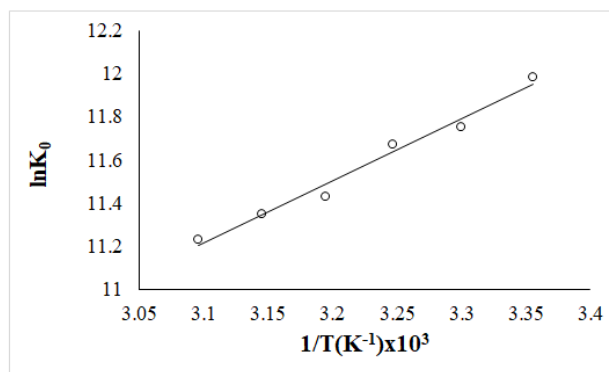


Figure 14. The plot of $\ln K_0$ vs $1/T$ for the enthalpy change of the biosorption process

increasing contact time, solution temperature and initial dye concentration. Biosorption equilibrium time is found to be 120 min. The pHzpc point of ASBP was determined as 6.62 and the pKa value of R-254 was found to be 8.46 from the literature. So, the pH value of the ASBP is chosen as 5.69, which is the initial solution pH value of ASBP in aqueous solutions since the q_e at the initial solution pH is about 4.97 mg.g^{-1} . The kinetic model best suited to the biosorption of R-254 on ASBP is found to be the pseudo second order model. The biosorption process fits well to

the Langmuir isotherm model. The maximum monolayer biosorption capacity is 84.75 mg.g⁻¹. The positive value of ΔH° (2.7 kJ.mol⁻¹) confirm that biosorption process is endothermic. The biosorption of R-254 onto ASBP is a spontaneous and thermodynamically favorable process at

all the experimental temperatures, since the values of ΔG° are negative. Consequently, ASBP can be used as a low-cost and efficient biosorbent in the removal of R-254 in industrial processes.

Nomenclature			
C ₀	Initially dye concentration (mg.L ⁻¹)	b _T	Isotherm constant of Temkin
C _e	Equilibrium dye concentration (mg.L ⁻¹)	ε	Dubinin–Radushkevich isotherm constant
C _t	Dye concentration at time t (mg.L ⁻¹)	ASBP	Activated sugar beet pulp
q _e	Biosorption capacity at time equilibrium (mg.g ⁻¹)	R _g	Gas constant (J.mol ⁻¹ .K ⁻¹)
q _t	Adsorbed amount at time t (mg.g ⁻¹)	T	Temperature (K)
q _{e,cal}	Calculated adsorption capacity (mg.g ⁻¹)	V	Volume (L)
q _{e,exp}	Experimental adsorption capacity (mg.g ⁻¹)	m	Biosorbent dosage (g)
k ₁	Rate constant for the pseudo-first kinetic model (min ⁻¹)	t	Time (min)
k ₂	Rate constant for the pseudo-second kinetic model (g.mg ⁻¹ .min ⁻¹)	K ₀	Adsorption equilibrium constant (-)
α	Elovich parameter (g.mg ⁻¹)	ΔG°	Free energy change of Gibbs (kJ.mol ⁻¹)
β	Elovich parameter (mg.g ⁻¹ .dk ⁻¹)	ΔH°	Enthalpy difference (kJ.mol ⁻¹)
k _{dif}	Rate coefficient of diffusion (mg.g ⁻¹ .min ^{-1/2})	ΔS°	Entropy difference (kJ.mol ⁻¹)
C	The intercept and relate to the thickness of the boundary layer	S	Surface Area(m ² .g ⁻¹)
R _L	The highest initial concentration (mg/L)	V _p	Pore Volume (cm ³ .g ⁻¹)
K _L	Langmuir coefficient (L.mg ⁻¹)		Average Por Size (nm)
K _f	Freundlich isotherm constant (mg.g ⁻¹)	d _p	
n	Freundlich isotherm constant (L.g ⁻¹)		
K _T	Tempkin isotherm equilibrium binding constant(L.g ⁻¹)		

References

Agarry S., and Ogunleye O. (2014). Chemically treated kola nut pod as low-cost natural adsorbent for the removal of 2, 4-dinitrophenol from synthetic wastewater: batch equilibrium, kinetic, and thermodynamic modelling studies, *Turkish Journal of Engineering and Environmental Sciences*, **38**, 11–40.

Akar S.T., Celik S., Tunc D., Balk Y.Y., and Akar T. (2016). Biosorption potential of surface-modified waste sugar beet pulp for the removal of Reactive Yellow 2 (RY2) anionic dye, *Chemical Engineering Journal*, **40**, 1044–1054.

Akar T., Celik S., and Akar S.T. (2010). Biosorption performance of surface modified biomass obtained from *Pyraacantha coccinea* for the decolorization of dye contaminated solutions, *Chemical Engineering Journal*, **160**, 466–472.

Aksu Z., and Isoglu I.A. (2005), Removal of copper (II) ions from aqueous solution by biosorption onto agricultural waste sugar beet pulp, *Process Biochemistry*, **40**, 3031–3044.

Altundogan H.S., Bahar N., Mujde B., and Tumen F. (2007). The use of sulphuric acid-carbonization products of sugar beet pulp in Cr (VI) removal, *Journal of hazardous materials*, **144**, 255–264.

Altundogan H.S. (2005). Cr (VI) removal from aqueous solution by iron (III) hydroxide-loaded sugar beet pulp, *Process Biochemistry*, **40**, 1443–1452.

Amri N., Radji S., Ghemati D., and Djamel A. (2019). Studies on equilibrium swelling, dye adsorption, and dynamic shear rheology of polymer systems based on chitosan-poly (vinyl alcohol) and montmorillonite. *Chemical Engineering Communications*, **206**, 716–730.

Bulut Y., and Aydin H. (2006). A kinetics and thermodynamics study of methylene blue adsorption on wheat shells. *Desalination*, **194**, 259–267.

Castro L., Blázquez M.L., González F., Muñoz J.A., and Ballester A. (2017). Biosorption of Zn (II) from industrial effluents using sugar beet pulp and *F. vesiculosus*: From laboratory tests to a pilot approach. *Science of the Total Environment*, **598**, 856–866.

Chemical book 2016. Pigment Red 254 Properties, https://www.chemicalbook.com/ChemicalProductProperty_EN_CB1323591.htm.

Danouche M., El Arroussi H., Bahafid W., and El Ghachtouli N. (2021). An overview of the biosorption mechanism for the bioremediation of synthetic dyes using yeast cells. *Environmental Technology Reviews*, **10**, 58–76.

Fathi MR., Asfaram A., and Farhangi A. (2015). Removal of Direct Red 23 from aqueous solution using corn stalks: isotherms, kinetics and thermodynamic studies, *Spectrochimica Acta Part A: Molecular and Biomolecular Spectroscopy*, **135**, 364–372.

Foroughi-Dahr M., Abolghasemi H., Esmaili M., Shojamoradi A., and Fatoorehchi H. (2015). Adsorption characteristics of Congo red from aqueous solution onto tea waste, *Chemical Engineering Communications*, **202**, 181–193.

Gunduz F., and Bayrak B. (2017). Biosorption of malachite green from an aqueous solution using pomegranate peel: equilibrium modelling, kinetic and thermodynamic studies, *Journal Molecular Liquids*. **243**, 790–798.

Harifi-Mood AR., and Hadavand-Mirzaie F. (2015). Adsorption of Basic violet 16 from aqueous solutions by waste sugar beet pulp: kinetic, thermodynamic, and equilibrium isotherm studies. *Chemical Special Bioavailable*, **27**, 8–14.

Imamoglu M., and Tekir O. (2008). Removal of copper (II) and lead (II) ions from aqueous solutions by adsorption on activated carbon from a new precursor hazelnut husks, *Desalination*, **228**, 108–113.

- Joseph O., Rouez M., Métivier-Pignon H., Bayard R., Emmanuel E., and Gourdon R. (2009). Adsorption of heavy metals on to sugar cane bagasse: Improvement of adsorption capacities due to anaerobic degradation of the biosorbent, *Environmental Technology*, **30**, 1371–1379.
- Kalkan N.A., Aksoy S., Aksoy E.A., and Hasirci N. (2012). Adsorption of reactive yellow 145 onto chitosan coated magnetite nanoparticles. *Journal Application Polymer Science*, **124**, 576–584.
- Kavci E. (2020). Malachite green adsorption onto modified pine cone: Isotherms, kinetics and thermodynamics mechanism. *Chemical Engineering Communications*, 1–10.
- Khattari S.D., and Singh M.K. (2009). Removal of malachite green from dye wastewater using neem sawdust by adsorption. *Journal Hazardous Materials*, **167**, 1089–1094.
- Lacin O., Haghghatnia A., Demir F., and Sevim F. (2019). Adsorption Characteristics and Behaviors of Natural Red Clay for Removal of BY28 from Aqueous Solutions. *International Journal Trend Science Research Development*, **3**, 1037–1047.
- Lafta A.J., Halbus A.F., Athab Z.H., Kamil A.M., Hussein A.S., Qhat A.F., and Hussein F.H. (2014). Effects of Activators on Adsorption Ability of Reactive Yellow-145 Dye on Activated Carbon from Iraqi Zahdi Date Palm Seeds, *Asian Journal Chemistry*, **26**.
- Li D., Yan J., and Liu Z. (2016). Adsorption kinetic studies for removal of methylene blue using activated carbon prepared from sugar beet pulp, *International Journal Environmental Science Technology*, **13**, 1815–1822.
- Malekbala M.R., Hosseini S., Yazdi S.K., Soltani S.M., and Malekbala M.R. (2012). The study of the potential capability of sugar beet pulp on the removal efficiency of two cationic dyes. *Chemical Engineering Research and Design*, **90**, 704–712.
- McKay G., Ho Y.S., and Ng J.C.Y. (1999). Biosorption of copper from waste waters: a review. *Separation Purification Methods*, **28**, 87–125.
- Ngah W.W., Teong L.C., Hanafiah M.A.K.M. (2011). Adsorption of dyes and heavy metal ions by chitosan composites: A review, *Carbohydrate Polymers*, **83**, 1446–1456.
- Nuhanović M., Grebo M., Draganović S., Memić M., and Smječanin N. (2019). Uranium (VI) biosorption by sugar beet pulp: equilibrium, kinetic and thermodynamic studies. *Journal Radioanalytical Nuclear Chemistry*, **322**, 2065–2078.
- Pehlivan E., Cetin S., and Yanik B.H. (2006). Equilibrium studies for the sorption of zinc and copper from aqueous solutions using sugar beet pulp and fly ash. *Journal Hazard Materials*, **135**, 193–199.
- Pehlivan E., Yanik B.H., Ahmetli G., and Pehlivan M. (2008). Equilibrium isotherm studies for the uptake of cadmium and lead ions onto sugar beet pulp. *Bioresource Technology*, **99**, 3520–3527.
- Pitsari S., Tsoufakis E., and Loizidou M. (2013). Enhanced lead adsorption by unbleached newspaper pulp modified with citric acid. *Chemistry Engineering Journal*, **223**, 18–30.
- Rafatullah M., Sulaiman O., Hashim R., and Ahmad A. (2010). Adsorption of methylene blue on low-cost adsorbents, a review. *Journal Hazard Materials*, **177**, 70–80.
- Rathi B.S., Kumar P.S., Vo D.V.N. (2021). Critical review on hazardous pollutants in water environment: Occurrence, monitoring, fate, removal technologies and risk assessment. *Science of The Total Environment*, **797**, 149134.
- Reddad Z., Gérente C., André Y., Ralet M.C., Thibault J.F., Le Cloirec P. (2002). Ni (II) and Cu (II) binding properties of native and modified sugar beet pulp. *Carbohydrate Polymer*, **49**, 23–31.
- Reynier N., Coudert L., Blais J.F., Mercier G., and Besner S. (2015). Treatment of contaminated soil leachate by precipitation, adsorption and ion Exchange, *Journal Environmental Chemistry Engineering*, **3**, 977–985.
- Salazar-Rabago J.J., Leyva-Ramos R., Rivera-Utrilla J., Ocampo-Perez R., and Cerino-Cordova F.J. (2017). Biosorption mechanism of Methylene Blue from aqueous solution onto white pine (*Pinus durangensis*) sawdust: effect of operating conditions. *Sustainable Environmental Research*, **27**, 32–40.
- Tay S.Y., Wong V.L., Lim S.S., and Teo I.L.R. (2020). Adsorption equilibrium, kinetics and thermodynamics studies of anionic methyl orange dye adsorption using chitosan-calcium chloride gel beads. *Chemical Engineering Communications*, 1–19.
- Tran H.N., You S.J., Nguyen T.V., and Chao H.P. (2017). Insight into the adsorption mechanism of cationic dye onto biosorbents derived from agricultural wastes. *Chemical Engineering Communications*, **204**, 1020–1036.
- Vučurović V.M., Razmovski R.N., and Tekić M.N. (2012). Methylene blue (cationic dye) adsorption onto sugar beet pulp: equilibrium isotherm and kinetic studies. *Journal of The Taiwan Institute of Chemical Engineers*, **43**, 108–111.
- Wang X.S., Liu X., Wen L., Zhou Y., Jiang Y., and Li Z. (2008). Comparison of basic dye crystal violet removal from aqueous solution by low-cost biosorbents. *Separation Science and Technology* **43**(14), 3712–3731.
- Wanyonyi W.C., Onyari J.M., and Shiundu P.M. (2014). Adsorption of Congo red dye from aqueous solutions using roots of *Eichhornia crassipes*: kinetic and equilibrium studies. *Energy Procedia*, **50**, 862–869.
- Yagub M.T., Sen T.K., Afroze S., and Ang H.M. (2014). Dye and its removal from aqueous solution by adsorption: a review. *Advance Colloid Interface Science*, **209**, 172–184.
- Yao Y., Gao B., Inyang M., Zimmerman A.R., Cao X., Pullammanappallil P., and Yang L. (2011). Removal of phosphate from aqueous solution by biochar derived from anaerobically digested sugar beet tailings. *Journal Hazardous Materials*, **190**, 501–507.
- Yusuf M., Khan S.A., Abul W., Sharma M. (2021). Current And Future Prospects Of Dye Confiscation Potential Of Inorganic-Based Materials: A Mini Review. *Asian Journal of Microbiology, Biotechnology and Environmental Sciences*, **23**(1), 89–95.
- Zhou X., Yu X., Hao J., and Liu H. (2022). Comments on the calculation of the standard equilibrium constant using the Langmuir model in *Journal of Hazardous Materials* 422 (2022) 126863. *Journal of Hazardous Materials*, **429**, 128407.
- Zhu M., Zhu L., Wang J., Yue T., Li R., and Li Z. (2017). Adsorption of Cd (II) and Pb (II) by in situ oxidized Fe₃O₄ membrane grafted on 316L porous stainless steel filter tube and its potential application for drinking water treatment. *Journal Environmental Management*, **196**, 127–136.
- Zou W., and Zhao L. (2012). Removal of uranium (VI) from aqueous solution using citric acid modified pine sawdust: batch and column studies. *Journal of Radioanalytical and Nuclear Chemistry*, **292**(2), 585–595.